Pergamon

Int. J. Solids Structures Vol. 35, Nos 31–32, pp. 4337–4350, 1998

0020-7683/98 $19.00 + .00

PII: S0020-7683(97)00319-3

INTERACTION OF WEDGE CRACK AND GRAIN BOUNDARY DISLOCATIONS

M. S. WU* and M. D. HE
Department of Engineering Mechanics, University of Nebraska-Lincoln, W317-4 Nebraska Hall, Lincoln, NE 68588-0526, U.S.A.

(*Received* 30 *October* 1996; *in revised form* 30 *May* 1997)

Abstract—Analysis of the interaction between a triple junction wedge crack and the pile-ups of grain boundary dislocations is used to investigate crack nucleation. Through the numerical solutions of a system of integral equations, the rearrangement of the dislocations and the stress redistribution due to the crack formation are fully taken into account in the analysis. Under remote tension, numerical results are obtained for the stress intensity factors, the dislocation populations on the grain boundaries, as well as the equilibrium crack lengths. The dependence of the crack length and the crack stability on the grain boundary orientations and the pile-up lengths is investigated. © 1998 Elsevier Science Ltd. All rights reserved.

1. INTRODUCTION

Wedge cracks at triple junctions are frequently observed in polycrystalline materials. In metals, the possible crack nucleation mechanisms can arise from the absorption and dissociation of lattice dislocations in grain boundaries, leading to (i) pile-ups of glissile extrinsic grain boundary dislocations (EGBDs) around triple junctions, (ii) singular or split disclinations at triple junctions, and (iii) disordered network of sessile grain boundary dislocations on grain boundary planes (Nazarov *et al.*, 1993). These structures are considered as the constituent elements of a non-equilibrium grain boundary, and have significant effects on the flow and fracture behavior of polycrystalline materials. For instance, Nazarov (1994) investigated the role of non-equilibrium grain boundaries in the yield and flow stress of polycrystals. Rybin and Zhukovskii (1978) analyzed crack nucleation due to a disclination mechanism, and Gutkin and Ovid'ko (1994) compared crack nucleation at a triple junction disclination to the local amorphization of the junction. Wu and Niu (1995) investigated crack nucleation due to the pile-ups of EGBDs at triple junctions in polycrystalline ice by a continuous modeling of the dislocations. Wu and Zhou (1996a) pursued a similar investigation using discrete dislocations. Picu and Gupta (1995) investigated crack nucleation is columnar ice due to the grain boundary sliding mechanism.

Various approximations are used in the above-mentioned crack nucleation studies. First, the redistribution of the EGBDs or disclination stress field by crack formation is ignored in calculating the stress intensity factors (SIFs). Second, an approximate model of a wedge nucleus formed by the EGBDs is used in the works of Wu and co-workers. The model assumes that all the EGBDs in the pile-ups enter the head of the wedge crack and that no redistribution of the EGBDs in the crack is possible. Smith and Barnby (1967) proposed a model that does take into account stress redistributions and the rearrangement of dislocations within a crack, but the model is restricted to a single shear crack interacting with a coplanar group of edge dislocations piling up against the head of the crack. Third, it is always assumed in the above-mentioned works that a wedge crack forms with a single branch on one grain boundary. The possibility of a crack with two or three branches along the grain boundaries is not considered.

This paper attempts to remove the above theoretical deficiencies, i.e., the stress redistribution caused by crack formation, and the interaction between EGBDs and wedge crack. A wedge crack of a single branch is considered, although multiple branches can also be

* Author to whom correspondence should be addressed. E-mail: wu@emwu.unl.edu.

analyzed without difficulty. A nucleation model is also proposed in which the EGBDs on a boundary coalesce to form a crack nucleus. The nucleus may extend under the wedging action of the EGBDs on the other two boundaries. The SIFs of the wedge crack under remote tension are numerically computed and used to determine the equilibrium length and the stability of the crack. A further analysis determines whether the nucleation of the crack is energetically favorable.

Certain assumptions remain in the present analysis. In particular, the local heterogeneity of the grains associated with their elastic or thermal anisotropy is not taken into account. Any image stresses due to the grain boundaries are neglected. The EGBDs are taken to be edge in character with their Burgers vectors tangential to the grain boundary planes. Also, the plane strain condition is assumed.

The theoretical approach is based on the continuous modeling of the EGBDs and the continuous dislocation modeling of the wedge crack. This is described in Section 2. The theory leads to a system of integral equations with the dislocation densities of the EGBDs and the real crack as unknowns. Section 2 also contains a description of the nucleation model. Numerical results of the SIFs obtained by solving the integral equations are presented in Section 3. The equilibrium crack lengths and the stability characteristics are also given in this section. Finally, a list of conclusions is provided in Section 4.

2. THEORETICAL MODELING

2.1. *Problem description*

Consider a wedge crack interacting with two groups of EGBDs on the grain boundary planes (see Fig. 1). A global x–y frame with origin at the triple junction is used for reference. The EGBDs pile up around the triple junction under a remote uniaxial tension σ_y^∞ in the y-direction. The grain boundaries to the right, upper left and lower left of the triple junction are denoted by 1, 2 and 3, respectively. Similarly, the grain boundary orientations with respect to the x-direction are denoted by θ_q, $q = 1, 2, 3$. The length of crack j is denoted by $\hat{l}_j$ ($\hat{l}_1$ is shown in Fig. 1). The sources of the EGBDs are located at the distances l_q from the triple junction. The distances l_q are thus equal to the pile-up lengths. Local coordinates s_k, $k = 1, 2, 3$ or t_q are used to describe positions within pile-up groups, while $\hat{s}_j$ or $\hat{t}_j$ are used to describe positions within the crack. The coordinates s_k and $\hat{s}_j$ refer to the positions at

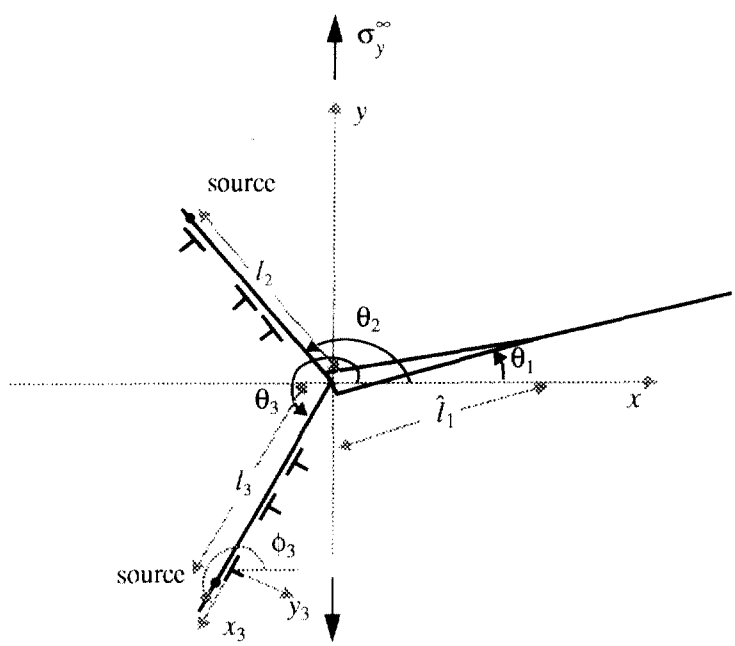

Fig. 1. The interaction between extrinsic grain boundary dislocations and a triple junction wedge crack.

which the forces or stresses are of interest, while t_q and $\hat{t}_j$ are the source points, i.e. the positions of the defects causing the forces or stresses. Furthermore, local frames x_q–y_q are attached to the EGBDs. The local orientations of the EGBDs are specified by ϕ_q with respect to the x-direction.

2.2. *Equilibrium conditions and boundary conditions*

Under the remote stress amplified by the crack, the continuously distributed EGBDs pile up in equilibrium around the triple junction. At each location s_k, $k = 1, 2, 3$ within the pile-up on boundary k, the shear stress due to the remote loading (S_k^{∞}) and the crack j ($\hat{F}_{jk}$, $j = 1, 2$ or $3, j \neq k$) acts on the EGBD distribution. This is balanced by the shear stress F_{qk}, $q = 1, 2, 3, q \neq j$ of all the EGBD distributions. The symbol S_k^{∞} denotes the resolved shear stress on boundary k. The contribution $\hat{F}_{jk}$ is a function of the dislocation strength density α_j of the crack and the positions s_k, where α_j is in general complex and has the unit of stress. The contribution F_{qk} is a function of the dimensionless dislocation densities ρ_q of the pile-ups and the positions s_k. The equilibrium conditions for the EGBDs on the boundaries k can then be written as:

$$\sum_{q=1, q\neq j}^{3} F_{qk}(\rho_q, s_k) + \hat{F}_{jk}(\alpha_j, s_k) + S_k^{\infty} = 0 \quad 0 < s_k < l_k; k \neq j. \tag{1}$$

Note that (1) actually consists of two equations corresponding to the equilibrium conditions for the two pile-ups on the two boundaries without the crack.

The crack, modeled as a continuous distribution of dislocations, is assumed to be traction-free. These dislocations are called crack dislocations in contrast to the physical dislocations (EGBDs). The normal and shear stresses on the crack j can be attributed to the crack dislocations on boundary j, the EGBDs on the other two boundaries and the remote stress. The normal stresses due to the three contributions are denoted by $\hat{N}_{jj}$, N_{qj} and N_j^{∞}, and the corresponding shear stresses by $\hat{S}_{jj}$, S_{qj} and S_j^{∞}. Summations of the normal and shear stresses on crack $j = 1, 2$ or 3 lead to:

$$\hat{N}_{jj}(\alpha_j, \hat{s}_j) + \sum_{q=1, q\neq j}^{3} N_{qj}(\rho_q, \hat{s}_j) + N_j^{\infty} = 0 \quad 0 < \hat{s}_j < \hat{l}_j, \tag{2}$$

$$\hat{S}_{jj}(\alpha_j, \hat{s}_j) + \sum_{q=1, q\neq j}^{3} S_{qj}(\rho_q, \hat{s}_j) + S_j^{\infty} = 0 \quad 0 < \hat{s}_j < \hat{l}_j. \tag{3}$$

Equations (1)–(3) constitute a system of four singular integral equations of the Cauchy type (see Section 2.4).

2.3. *Stress field of dislocation groups*

The stress field of dislocation groups can be derived from that of a discrete edge dislocation in an infinite body. It is most convenient to write down the relevant stresses using the method of complex functions. Specifically, consider the complex variable $z = x + iy$, where $i = \sqrt{-1}$ and x, y are the global coordinates indicated in Fig. 1. The circumferential and shear stresses $\sigma_{\theta\theta} + i\sigma_{r\theta}$ in the usual polar frame r–θ can be written in terms of the complex function $\Phi(z)$ and $\Psi(z)$ as follows (Muskhelishvili, 1953):

$$\sigma_{\theta\theta} + i\sigma_{r\theta} = \Phi(z) + \overline{\Phi(z)} + e^{2i\theta}[\bar{z}\Phi'(z) + \Psi(z)], \tag{4}$$

where e is the exponential, the overhead bar denotes complex conjugation, and the prime denotes differentiation with respect to the argument. The complex functions for the case of a discrete edge dislocation at $z = z_0$ are given by:

$$\Phi(z) = \frac{\alpha}{(z-z_0)}, \quad \Psi(z) = \frac{\bar{\alpha}}{z-z_0} + \frac{\alpha \bar{z_0}}{(z-z_0)^2}, \tag{5}$$

where

$$\alpha = \mu b\, e^{i\phi}/\pi i(\kappa+1) \tag{6}$$

is the strength of the dislocation. In (6), b is the Burgers vector magnitude, ϕ is the orientation of the dislocation, μ is the shear modulus, and $\kappa = 3-4\nu$ for plane strain; ν being the Poisson's ratio.

Consider an EGBD with local orientation ϕ_q and Burgers vector magnitude b_q. Suppose it is located at $z = z_0$ on grain boundary q so that $z_0 = t_q\, e^{i\theta_q}$. The shear and circumferential stresses are needed at some location z on a boundary. The location z can be that of another EGBD on boundary k in which case $z = s_k\, e^{i\theta_k}$, or a crack dislocation on boundary j, in which case $z = \hat{s}_j\, e^{i\theta_j}$. Substituting (5) in (4), the circumferential and shear stresses on boundary k or j can be derived after some algebraic manipulation. If z is the location of the second EGBD with orientation ϕ_k, then the stress components are written in the local frame of the second EGBD. This is achieved by setting 2θ in (4) equal to $2\phi_k$. Then, the stresses can be expressed in terms of t_q, s_k, θ_q, θ_k, ϕ_q and ϕ_k as:

$$\sigma_{\theta\theta}(t_q, s_k; \theta_q, \theta_k; \phi_q; \theta = \phi_k) + i\sigma_{r\theta}(t_q, s_k; \theta_q, \theta_k; \phi_q; \theta = \phi_k) = \frac{D}{2}\left(\frac{A+\bar{A}+B}{F_1} + \frac{C+E}{F_2}\right), \tag{7}$$

where

$$D = \frac{2\mu b_q}{\pi(\kappa+1)}, \tag{8}$$

$$F_1 = s_k^2 + t_q^2 - 2s_k t_q \cos(\theta_q - \theta_k), \tag{9}$$

$$F_2 = s_k^4 + t_q^4 + 4s_k^2 t_q^2 - 4s_k t_q (s_k^2 + t_q^2)\cos(\theta_k - \theta_q) + 2s_k^2 t_q^2 \cos(2\theta_k - 2\theta_q), \tag{10}$$

$$A = [s_k \sin(\phi_q - \theta_k) - t_q \sin(\phi_q - \theta_q)] - i[s_k \cos(\phi_q - \theta_k) - t_q \cos(\phi_q - \theta_q)], \tag{11}$$

$$B = [s_k \sin(\theta_k + \phi_q - 2\phi_k) - t_q \sin(\theta_q + \phi_q - 2\phi_k)] + i[s_k \cos(\theta_k + \phi_q - 2\phi_k) - t_q \cos(\theta_q + \phi_q - 2\phi_k)], \tag{12}$$

$$\begin{aligned} C = s_k[&s_k^2 \sin(3\theta_k - \phi_q - 2\phi_k) + t_q^2 \sin(2\theta_q + \theta_k - \phi_q - 2\phi_k) \\ &- 2s_k t_q \sin(2\theta_k + \theta_q - \phi_q - 2\phi_k)] + is_k[s_k^2 \cos(3\theta_k - \phi_q - 2\phi_k) \\ &+ t_q^2 \cos(2\theta_q + \theta_k - \phi_q - 2\phi_k) - 2s_k t_q \cos(2\theta_k + \theta_q - \phi_q - 2\phi_k)], \end{aligned} \tag{13}$$

$$\begin{aligned} E = t_q[&s_k^2 \sin(\phi_q - \theta_q - 2\theta_k + 2\phi_k) + t_q^2 \sin(\phi_q - 3\theta_q + 2\phi_k) \\ &- 2s_k t_q \sin(\phi_q - 2\theta_q - \theta_k + 2\phi_k)] - it_q[s_k^2 \cos(\phi_q - \theta_q - 2\theta_k + 2\phi_k) \\ &+ t_q^2 \cos(\phi_q - 3\theta_q + 2\phi_k) - 2s_k t_q \cos(\phi_q - 2\theta_q - \theta_k + 2\phi_k)], \end{aligned} \tag{14}$$

and $\bar{A}$ is the complex conjugate of A. Note that D, F_1 and F_2 are real. If z is a point on the crack, 2θ in (4) equals $2\theta_j$ since the stresses in (2) and (3) are to be added in the polar coordinates determined by the grain boundary orientations θ_j. Also, s_k in (7)–(14) should

be replaced by $\hat{s}_j$, the location of the crack dislocation on boundary j. Then the stress components can be expressed as:

$$\sigma_{\theta\theta}(t_q, \hat{s}_j; \theta_q, \theta_j; \phi_q; \theta = \theta_j) + i\sigma_{r\theta}(t_q, \hat{s}_j; \theta_q, \theta_j; \phi_q; \theta = \theta_j) = \frac{D}{2}\left(\frac{A+\bar{A}+B}{F_1} + \frac{C+E}{F_2}\right), \tag{15}$$

where θ_j replaces ϕ_k in F_1, F_2, A, $\bar{A}$, B, C and E [see (9)–(14)]. Equation (7) or (15) gives the stress field of a single EGBD of Burgers vector b_q. For a continuous distribution of density ρ_q on boundary q, (7) and (15) should be replaced by:

$$\sigma_{\theta\theta} + i\sigma_{r\theta} = \int_0^{t_q} \frac{\mu\rho_q}{\pi(\kappa+1)}\left(\frac{A+\bar{A}+B}{F_1} + \frac{C+E}{F_2}\right) dt_q, \tag{16}$$

in which $\rho_q\, dt_q$ replaces b_q of (8). Note that ρ_q is an unknown function of t_q.

Consider next a crack dislocation located at $z = z_0$ on a grain boundary j. The shear and circumferential stresses are needed at some location z on a boundary. In this case, $z_0 = \hat{t}_j e^{i\theta_j}$ and $z = s_k e^{i\theta_k}$ (for EGBD location) or $z = \hat{s}_j e^{i\theta_j}$ (for second crack dislocation). Equation (5) can also be substituted in (4) to obtain the stresses. The strength $\alpha_j = \alpha_{Rj} + i\alpha_{Ij}$ rather than the density ρ_q of (16) is chosen as the unknown. The circumferential and shear stresses at the location of an EGBD (orientation ϕ_k) on boundary k can be expressed in terms of $\hat{t}_j$, s_k, θ_j, θ_k, α_j and ϕ_k as:

$$\sigma_{\theta\theta}(\hat{t}_j, s_k; \theta_j, \theta_k; \alpha_j, \theta = \phi_k) + i\sigma_{r\theta}(\hat{t}_j, s_k; \theta_j, \theta_k; \alpha_j, \theta = \phi_k) = \frac{G+\bar{G}+H}{F_1} + \frac{P-Q}{F_2}, \tag{17}$$

where

$$G = [(s_k\cos\theta_k - \hat{t}_j\cos\theta_j)\alpha_{Rj} + (s_k\sin\theta_k - \hat{t}_j\sin\theta_j)\alpha_{Ij}] + i[(s_k\cos\theta_k - \hat{t}_j\cos\theta_j)\alpha_{Ij} - (s_k\sin\theta_k - \hat{t}_j\sin\theta_j)\alpha_{Rj}], \tag{18}$$

$$H = (s_k\cos(2\phi_k - \theta_k) - \hat{t}_j\cos(2\phi_k - \theta_j))\alpha_{Rj} + (s_k\sin(2\phi_k - \theta_k) - \hat{t}_j\sin(2\phi_k - \theta_j))\alpha_{Ij} + i[-(s_k\cos(2\phi_k - \theta_k) - \hat{t}_j\cos(2\phi_k - \theta_j))\alpha_{Ij} + (s_k\sin(2\phi_k - \theta_k) - \hat{t}_j\sin(2\phi_k - \theta_j))\alpha_{Rj}], \tag{19}$$

$$\begin{aligned} P = {} & [s_k^2\cos(2\phi_k - 2\theta_k - \theta_j) + \hat{t}_j^2\cos(2\phi_k - 3\theta_j) - 2s_k\hat{t}_j\cos(2\phi_k - 2\theta_j - \theta_k)]\alpha_{Rj}\hat{t}_j \\ & - [s_k^2\sin(2\phi_k - 2\theta_k - \theta_j) + \hat{t}_j^2\sin(2\phi_k - 3\theta_j) - 2s_k\hat{t}_j\sin(2\phi_k - 2\theta_j - \theta_k)]\alpha_{Ij}\hat{t}_j \\ & + i([s_k^2\sin(2\phi_k - 2\theta_k - \theta_j) + \hat{t}_j^2\sin(2\phi_k - 3\theta_j) - 2s_k\hat{t}_j\sin(2\phi_k - 2\theta_j - \theta_k)]\alpha_{Rj}\hat{t}_j \\ & + [s_k^2\cos(2\phi_k - 2\theta_k - \theta_j) + \hat{t}_j^2\cos(2\phi_k - 3\theta_j) - 2s_k\hat{t}_j\cos(2\phi_k - 2\theta_j - \theta_k)]\alpha_{Ij}\hat{t}_j), \end{aligned} \tag{20}$$

$$\begin{aligned} Q = {} & [\hat{t}_j^2\cos(2\phi_k - 2\theta_j - \theta_k) + s_k^2\cos(2\phi_k - 3\theta_k) - 2s_k\hat{t}_j\cos(2\phi_k - 2\theta_k - \theta_j)]\alpha_{Rj}s_k \\ & - [\hat{t}_j^2\sin(2\phi_k - 2\theta_j - \theta_k) + s_k^2\sin(2\phi_k - 3\theta_k) - 2s_k\hat{t}_j\sin(2\phi_k - 2\theta_k - \theta_j)]\alpha_{Ij}s_k \\ & + i([\hat{t}_j^2\sin(2\phi_k - 2\theta_j - \theta_k) + s_k^2\sin(2\phi_k - 3\theta_k) - 2s_k\hat{t}_j\sin(2\phi_k - 2\theta_k - \theta_j)]\alpha_{Rj}s_k \\ & + [\hat{t}_j^2\cos(2\phi_k - 2\theta_j - \theta_k) + s_k^2\cos(2\phi_k - 3\theta_k) - 2s_k\hat{t}_j\cos(2\phi_k - 2\theta_k - \theta_j)]\alpha_{Ij}s_k). \end{aligned} \tag{21}$$

When z denotes the location of a second dislocation on boundary j, then the stresses at z can be written as:

$$\sigma_{\theta\theta}(\hat{t}_j, \hat{s}_j; \theta_j, \theta_j : \alpha_j, \theta = \theta_j) + i\sigma_{r\theta}(\hat{t}_j, \hat{s}_j; \theta_j, \theta_j; \alpha_j, \theta = \theta_j) = \frac{G+\bar{G}+H}{F_1} + \frac{P-Q}{F_2}, \quad (22)$$

where ϕ_k in (17)–(21) is replaced by θ_j. For a continuous distribution of crack dislocations on boundary j, (17) and (22) should be replaced by:

$$\sigma_{\theta\theta} + i\sigma_{r\theta} = \int_0^{l_j} \left(\frac{G+\bar{G}+H}{F_1} + \frac{P-Q}{F_2} \right) \mathrm{d}\hat{t}_j. \quad (23)$$

The variable α_j in (17)–(23) should now be interpreted as the strength density with the unit of stress. Finally, it is noted that ϕ_j and ϕ_k can be set equal to θ_j and θ_k, respectively, in all the above equations without loss of generality since the EGBD orientation and the grain boundary orientation are either the same or differ by π. The difference of π will be reflected in the sign of the predicted dislocation density.

2.4. *Integral equations and additional conditions*

Substitution of (16) and (23) in the equilibrium and boundary conditions (1)–(3) yields a system of singular integral equations of the Cauchy type. For a crack on boundary j, the four equations can be written as:

$$\sum_{q=1, q\neq j}^{3} \int_0^{l_q} \frac{\mu\rho_q}{\pi(\kappa+1)} \mathrm{Im}\left(\frac{B(t_q, s_k)}{F_1(t_q, s_k)} + \frac{C(t_q, s_k) + E(t_q, s_k)}{F_2(t_q, s_k)} \right) \mathrm{d}t_q$$

$$+ \int_0^{\hat{l}_j} \mathrm{Im}\left(\frac{H(\hat{t}_j, s_k; \alpha_j)}{F_1(\hat{t}_j, s_k)} + \frac{P(\hat{t}_j, s_k; \alpha_j) - Q(\hat{t}_j, s_k; \alpha_j)}{F_2(\hat{t}_j, s_k)} \right) \mathrm{d}\hat{t}_j + S_k^{\infty} = 0,$$

$$0 < s_k < l_k, \quad k = 1, 2, 3; \quad k \neq j, \quad (24)$$

$$\int_0^{\hat{l}_j} \mathrm{Re}\left(\frac{2G(\hat{t}_j, \hat{s}_j; \alpha_j) + H(\hat{t}_j, \hat{s}_j; \alpha_j)}{F_1(\hat{t}_j, \hat{s}_j)} + \frac{P(\hat{t}_j, \hat{s}_j; \alpha_j) - Q(\hat{t}_j, \hat{s}_j; \alpha_j)}{F_2(\hat{t}_j, \hat{s}_j)} \right) \mathrm{d}\hat{t}_j$$

$$+ \sum_{q=1, q\neq j}^{3} \int_0^{l_q} \frac{\mu\rho_q}{\pi(\kappa+1)} \mathrm{Re}\left(\frac{2A(t_q, \hat{s}_j) + B(t_q, \hat{s}_j)}{F_1(t_1, \hat{s}_j)} + \frac{C(t_q, \hat{s}_j) + E(t_q, \hat{s}_j)}{F_2(t_q, \hat{s}_j)} \right) \mathrm{d}t_q + N_j^{\infty} = 0,$$

$$0 < \hat{s}_j < \hat{l}_j, \quad j = 1, 2 \quad \text{or } 3. \quad (25)$$

$$\int_0^{\hat{l}_j} \mathrm{Im}\left(\frac{H(\hat{t}_j, \hat{s}_j; \alpha_j)}{F_1(\hat{t}_j, \hat{s}_j)} + \frac{P(\hat{t}_j, \hat{s}_j; \alpha_j) - Q(\hat{t}_j, \hat{s}_j; \alpha_j)}{F_2(\hat{t}_j, \hat{s}_j)} \right) \mathrm{d}\hat{t}_j + \sum_{q=1, q\neq j}^{3} \int_0^{l_q} \frac{\mu\rho_q}{\pi(\kappa+1)}$$

$$\times \mathrm{Im}\left(\frac{B(t_q, \hat{s}_j)}{F_1(t_q, \hat{s}_j)} + \frac{C(t_q, \hat{s}_j) + E(t_q, \hat{s}_j)}{F_2(t_q, \hat{s}_j)} \right) \mathrm{d}t_q + S_j^{\infty} = 0, \quad 0 < \hat{s}_j < \hat{l}_j, \quad j = 1, 2 \quad \text{or } 3, \quad (26)$$

where "Re" and "Im" denote the real and imaginary parts, respectively. Also, S_k^{∞} in (24) is the shear stress transformed using the local dislocation orientation ϕ_k, while N_j^{∞}, S_j^{∞} are the normal and shear stresses transformed using the grain boundary orientations θ_j. The unknown functions are ρ_q and α_{Rj} and α_{Ij}. It can be shown that the singular terms of the integral equations are of the forms $1/(s_q - t_q)$ and $1/(\hat{s}_j - \hat{t}_j)$.

Equations (24)–(26) can be normalized to the intervals $-1 \leqslant t_q', s_k' \leqslant 1$ and $-1 \leqslant \hat{t}_j', \hat{s}_j' \leqslant 1$ by using

$$t_q = \frac{l_q}{2}(1+t'_q), \quad \hat{t}_j = \frac{\hat{l}_j}{2}(1+\hat{t}'_j), \tag{27}$$

and similar equations for s'_k and $\hat{s}'_j$. Then, the method of Gerasoulis (1982), which has been applied to solving singular integral equations in kinked crack problems, is adopted. The method involves writing the unknown densities as the product between a weight function w and certain unknown regular functions f_q, f_{Rj}, and f_{Ij}, i.e.,

$$\rho_q(t'_q) = \frac{f_q(t'_q)}{(1-t'_q)^{1/2}(1+t'_q)^{1/2}}, \quad \alpha_{Rj}(\hat{t}'_j)+i\alpha_{Ij}(\hat{t}'_j) = \frac{f_{Rj}(\hat{t}'_j)+if_{Ij}(\hat{t}'_j)}{(1-\hat{t}'_j)^{1/2}(1+\hat{t}'_j)^{1/2}}. \tag{28}$$

The one-half singularity is built into the weight function at the extremities of the cracks and the pile-ups. Strictly speaking, the singularity assumptions at both ends of the pile-ups and at the head of the crack may be incorrect. The method, however, relies on the use of the regular functions and certain additional conditions to numerically correct these assumptions as explained below.

The regular functions f_q, f_{Rj} and f_{Ij} are approximated by piecewise quadratic polynomials which are substituted in the integral equations. If the range $[-1, 1]$ is divided into R intervals, then the unknowns become the values of the regular functions at the $R+1$ boundary points of the range $[-1, 1]$. When these quadratic polynomials are divided by $(1-t'^2_q)^{1/2}$ or $(1-\hat{t}'^2_j)^{1/2}$, exact integrations can be carried out in (24)–(26). Collocation at R points within the intervals then leads to a system of R linear algebraic equations with $R+1$ unknowns. In total, there are $4R$ equations in $4(R+1)$ unknowns. An excess of four unknowns requires an equal number of additional equations.

The first two additional conditions are obtained by taking the functions f_q at the two sources on the boundaries without the crack to be zero, i.e.,

$$f_q(1) = 0 \quad q = 1, 2, 3; \quad q \neq j. \tag{29}$$

These conditions are intended to remove the singularity of $\rho_q(t'_q)$ at $t'_q = 1$, since no singularity is expected at the sources (see, e.g., Hirth and Lothe (1982) for the results of a stressed single pile-up). In (28), the function $\rho_q(t'_q)$ is written in the same form as $\alpha_{Rj}(\hat{t}'_j)+i\alpha_{Ij}(\hat{t}'_j)$ in order to simplify the numerical scheme for solving the system of integral equations. All numerical results show that $\lim_{t'_q \to 1} \rho_q(t'_q) = 0$, confirming that the singularity is effectively removed in the numerical calculations. The conditions $\rho_q(1) = 0$ were directly used by Vladimirov and Khanhanov (1969) in their discrete-continuous examination of dislocation pile-ups.

The next two additional conditions are derived from the analogy with kinked cracks. The singularities at the head of the crack may not be equal to one-half as assumed in (28). The crack, however, can be visualized as a kink wedged open by EGBDs. The usual treatment is to ignore the integration point at the head of the kink. This is effected by setting f_{Rj} and f_{Ij} to zero at this point (e.g., Lo, 1978; He and Hutchinson, 1989):

$$f_{Rj}(-1) = 0, \quad f_{Ij}(-1) = 0, \quad j = 1, 2 \quad \text{or } 3. \tag{30}$$

Unlike (29), (30) does not necessarily imply that $\alpha_{Rj}(-1)+i\alpha_{Ij}(-1) = 0$. Numerically, it is found that $\lim_{\hat{t}'_j \to -1}[\alpha_{Rj}(\hat{t}'_j)+i\alpha_{Ij}(\hat{t}'_j)] \neq 0$. The two sets of conditions (29) and (30) together yield four additional equations.

The singularities at the heads of the pile-ups are taken to be one-half and the regular functions f_q are relied upon to numerically correct the assumptions where necessary. No additional conditions are used. The singularity at the crack tip is assumed to be one-half. The effectiveness by which the regular functions correct the assumptions increases if the number of collocation points increases. Niu and Wu (1997) showed that in the case of strongly interacting kinked cracks R should be at least 160 for good accuracy.

If the sign of the remote uniaxial loading is changed, it can be seen from (24)–(26) that the solutions ρ_q, α_{Rj} and α_{Ij} will reverse their signs. Consequently, the SIFs will also reverse their signs. Thus, a negative K_I can arise in some cases, implying the possibility of closed cracks and frictional sliding. The issue will not be addressed in this paper. It should be mentioned, however, that an approximate treatment in crack nucleation models is to set K_I to zero when it is negative and to assume that the crack nucleates under a pure mode II condition (e.g., Wu and Niu, 1995).

To link the continuous approach to the discrete approach, the following non-integer dislocation population n_q can be defined:

$$\int_0^{l_q} \rho_q \, \mathrm{d}t_q = n_q b_q, \tag{31}$$

where $q = 1, 2, 3$; $q \neq j$ and the repeated subscripts do not imply summation. Negative values of n_q imply that the dislocations have negative Burgers vectors. The populations can be determined after the dislocation densities have been determined.

Once f_{Rj} and f_{Ij} are obtained, the mode I and mode II stress intensity factors K_I^j and K_{II}^j, $j = 1, 2$, or 3 can be computed from the stresses near and outside the cracks. The only non-vanishing contribution comes from the singular stresses of the crack dislocations associated with the crack itself. Consequently, letting $s_j \to \hat{l}_j$ from outside the crack and converting to normalized units, the stress intensity factors can be written as:

$$\begin{aligned} K_I^j + iK_{II}^j &= \lim_{s_j \to \hat{l}_j} \sqrt{2\pi(s_j - \hat{l}_j)} \int_0^{\hat{l}_j} \left[\mathrm{Re}\left(\frac{2G+H}{F_1} + \frac{P-Q}{F_2} \right) + i \, \mathrm{Im}\left(\frac{H}{F_1} + \frac{P-Q}{F_2} \right) \right]_{\hat{t}_j = s_j, \theta_j} \mathrm{d}\hat{t}_j \\ &= \sqrt{(2\hat{l}_j \pi^3)} \, e^{i\theta_j} [f_{Rj}(1) - i f_{Ij}(1)]. \end{aligned} \tag{32}$$

2.5. *Equilibrium crack length and nucleation model*

For plane strain, the equilibrium crack length can be determined from the solution to the following equation:

$$\frac{\partial E_c}{\partial \hat{l}} = 2\gamma - \mathscr{G} = 2\gamma - \left[\frac{(K_I^j)^2 + (K_{II}^j)^2}{2\mu/(1-\nu)} \right] = 0, \tag{33}$$

where E_c is the energy of the crack system, $\hat{l}$ is the crack length, 2γ the surface energy per unit length, $\mathscr{G}$ the energy release rate, μ the shear modulus, and ν the Poisson's ratio. Multiple solutions to (33) may exist. A crack is stable if it satisfies $\partial^2 E_c / \partial \hat{l}^2 > 0$. It is unstable if $\partial^2 E_c / \partial \hat{l}^2 < 0$.

To determine whether the nucleation of the crack with length predicted by (33) is energetically favorable, the following nucleation model is proposed. Under remote loading, EGBDs are generated by three sources located at the distances l_q from the triple junction. They pile up around the junction with group energy E_q. Analysis of the pile-ups in the absence of cracks is carried out using (1), which now consists of three equations with $k = 1$, 2 and 3. The conditions $q \neq j$ and $k \neq j$ become irrelevant. The EGBDs on one of the three boundaries, however, may coalesce to form a crack nucleus. The nucleus may extend under the wedging action of the EGBDs on the other two boundaries. Work is done during the coalescence of the EGBDs, and this is estimated as the work W required to move an equivalent superdislocation from the center of gravity of the pile-up to the triple junction. The Burgers vector magnitude of the superdislocation equals the integral of the dislocation density on the boundary. The nucleation of a crack is favorable if

$$E_q - E_c > 0. \tag{34}$$

Integration of (33) leads to $E_c = 2\gamma\hat{l} - \int_0^{\hat{l}} \mathcal{G}\, d\hat{l}$ plus an integration constant which should be equal to $E_q - W$. Therefore, (34) becomes:

$$E_q - E_c = \int_0^{\hat{l}} \mathcal{G}\, d\hat{l} - 2\gamma\hat{l} + W > 0, \tag{35}$$

where the lower limit of the integral corresponds to the size of the crack nucleus and is approximated as zero.

3. NUMERICAL RESULTS

3.1. *Physical and numerical model parameters*

As an example, parameter values appropriate for polycrystalline aluminum are chosen. The shear modulus and the Poisson's ratio are $\mu = 26.0$ GPa and $\nu = 0.347$. To compute n_q using (31), the Burgers vector magnitude of all the EGBDs is taken to be $b_q = b = 2.1 \times 10^{-10}$ m. In general, b_q depends on the crystallographic details of the adjoining grains. Also, a mean grain boundary length $l_0 = 50$ μm is assumed. A remote uniaxial tensile stress σ_∞^∞ of magnitude 20 MPa is applied. Furthermore, the following reference parameters for l_q and $\hat{l}_j$ are defined. For $q, j = 1, 2, 3$, $l_q = 0.15\ l_0$ and $\hat{l}_j = 10^4\ b = 2.1$ μm $= 0.042\ l_0$. The values of l_q are varied from $\sim 0.015\ l_0$–$0.15\ l_0$, i.e., the sources are close to the triple junction. Values of $\hat{l}_j$ up to approximately l_0 are considered. Reference values for the boundary orientations are $\theta_1 = 10^\circ$, $\theta_2 = 120^\circ$ and $\theta_3 = 240^\circ$.

Comparison of the stress intensity factors computed using $R = 60$, 180 and 240 show that numerical convergence is attained at $R = 240$ for all variations of the physical parameters considered. Convergence is less rapid for very short crack lengths, and is faster for mode I SIFs than for mode II SIFs. All results presented in this paper are generated with $R = 240$.

3.2. *Dependence of SIFs and dislocation populations on grain boundary orientations*

Consider a single crack on boundary 2. The dependence of the SIFs and n_q on the variation of θ_q are shown, respectively, on the left and right columns of Fig. 2. Note that θ_1 is varied from 0–90°, θ_2 from 90–180°, and θ_3 from 180–270°. In each variation, reference values of all the other parameters are used.

The dependence of K_I and K_II on θ_q is complex. Both SIFs change sign as θ_1 and θ_3 increase through 90°. The dependence on θ_2, the orientation of the boundary containing the crack, is less significant compared to the dependence on θ_1 and θ_3. The SIFs display extrema in the variations with θ_1 and θ_3 but not with θ_2. The implication is that certain combinations of boundary orientations can be more favorable for crack nucleation and growth. The largest amplitude of the mode I or mode II SIF in this example is approximately 0.5 MPa $\sqrt{\text{m}}$. Furthermore, the dislocation populations are predicted to vary between 0 and 300, depending on θ_q. The peak values of K_I and K_II do not necessarily correlate directly with the peak values of n_1 and n_3. This suggests that crack nucleation or growth can be associated with relatively small pile-up populations.

3.3. *Dependence of SIFs and dislocation populations on pile-up lengths and crack length*

The dependence of the SIFs of a boundary 2 crack on l_1 and l_3 (normalized by l_0) as well as its own length $\hat{l}_2$ (normalized by b) are shown on the left column of Fig. 3. The predicted dislocation populations are shown on the right column of Fig. 3. Except for the variations of the lengths shown on the horizontal axes, all other parameters assume their reference values.

At first observation is that the amplitude of K_I decreases, whereas K_II increases, with l_1 or l_3. In general, the details of the dependence of the SIFs on l_q depend on the boundary on which the crack is located. It can however be concluded that longer pile-ups do not

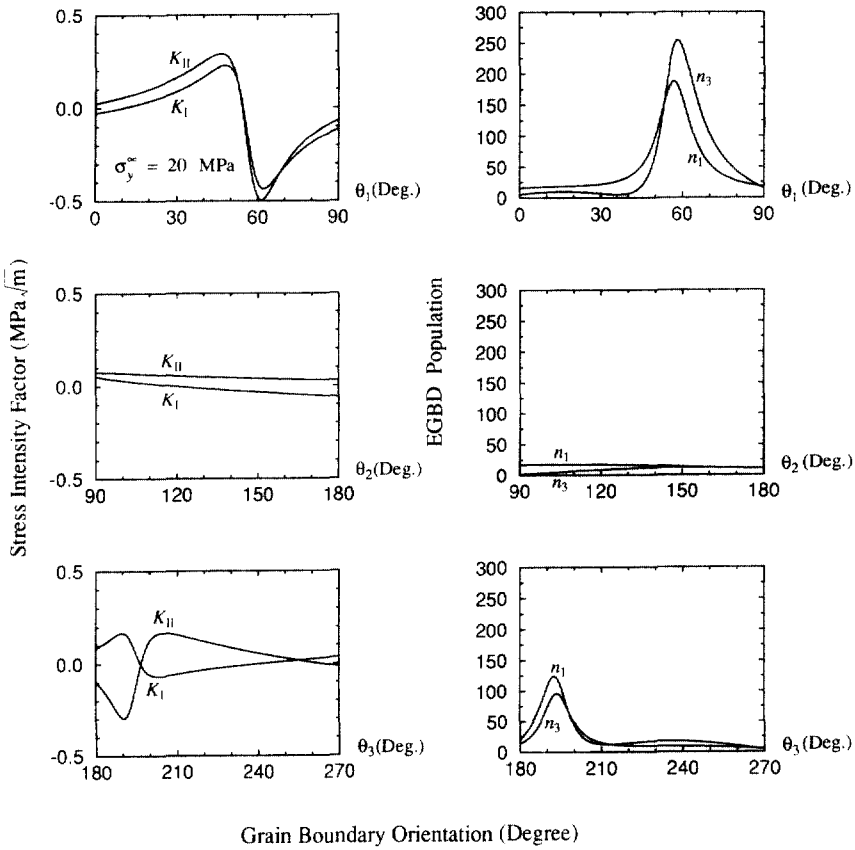

Fig. 2. Variations of the stress intensity factors and the dislocation populations n_1 and n_3 (non-integers) with the grain boundary orientations θ_1, θ_2 and θ_3. The crack is on boundary two.

necessarily imply larger SIFs. Both K_I and K_{II} decrease with $\hat{l}_2$ generally, as expected for a wedge crack. For moderately long cracks ($\log(\hat{l}_2/b) > 3.5$) K_I increases with $\hat{l}_2$, however. This reflects the increasing dominance of the remote tension as the crack lengthens. Furthermore, the plots of the dislocation populations suggest that no simple relations exist between the variations of the populations with variations of the SIFs. For instance, a decreasing K_I with l_3 is associated with increasing populations. Finally, it is seen that the dislocation populations on boundaries 1 and 3 decrease with $\hat{l}_2$, i.e., the dislocations are predicted to either enter and rearrange within the crack or reabsorb at the grain boundary sources. The increasing populations at large $\hat{l}_2$, on the other hand, show the complex interaction between the remote tension, pile-ups and crack.

3.4. *Equilibrium crack lengths and stability characteristics*

The crack is assumed to nucleate on boundary 2. The normalized crack length $\log(\hat{l}_2/b)$ is plotted against θ_1, θ_2, θ_3 and l_1/l_0, l_3/l_0 in Fig. 4. For each parameter that is varied, the other parameters are kept at the reference values except for the crack length which is predicted using (33). Four classes of crack length solutions are predicted: stable, unstable, energetically unfavorable, and non-existence.

A multiplicity of solutions may exist at certain combinations of grain boundary orientations. For instance, for a given θ_1 two solutions exist in the range $30^\circ < \theta_1 < 60^\circ$. The smaller and larger solutions are predicted to be either (i) stable and unstable, (ii) stable and energetically unfavorable, or (iii) unstable and stable. Also, the two solutions appear to converge to the same value at $\theta_1 \sim 45^\circ$ and then diverge after this value. Within the range $0^\circ < \theta_1 < 90^\circ$, $\hat{l}_2$ varies between $10^{0.3}$ and $10^{5.3}b$, or between 0.000419 and 41.9 μm. The smaller value is close to $2b$. This small value, predicted by the continuum theory, should be interpreted as an approximation of the crack length. In the variation of θ_3, a

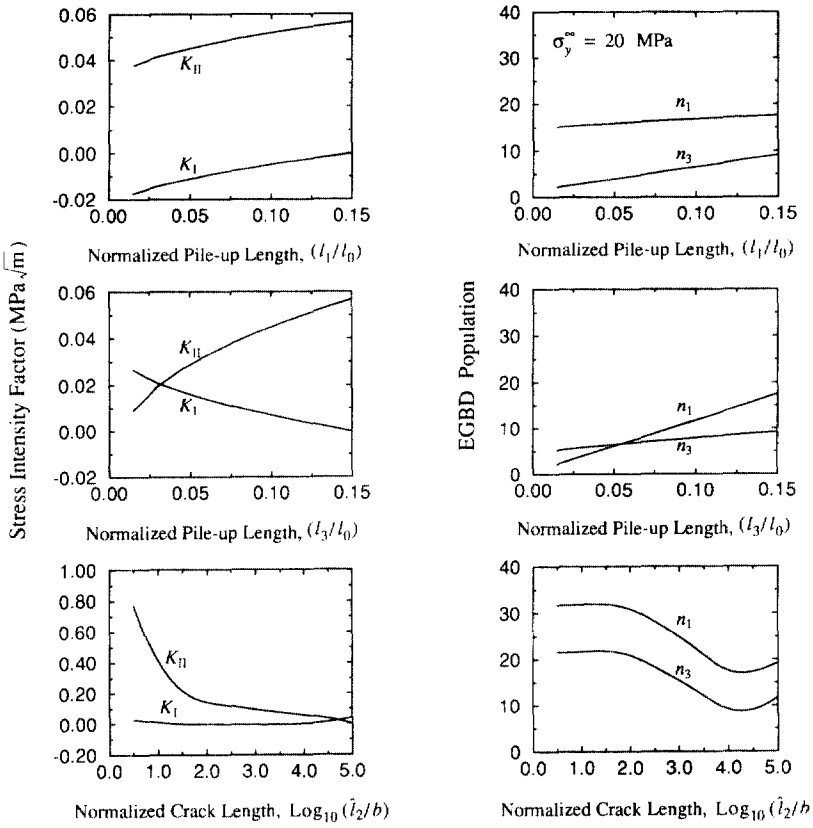

Fig. 3. Variations of the stress intensity factors and the dislocation populations n_1 and n_3 (non-integers) with the pile-up length l_1, l_3 and the crack length $\hat{l}_2$. The crack is on boundary two.

maximum of three solutions or no solutions at all are predicted. For instance, in the range $190^\circ < \theta_3 < 220^\circ$, the single, pair or triplet of solutions are found to be either (i) energetically unfavorable and stable, (ii) stable, (iii) stable, energetically unfavorable, stable, or (iv) stable and energetically unfavorable. No solutions are found at $\theta_3 = 260^\circ$ or 270°. Note that $\hat{l}_2$ also varies through five orders of magnitude as θ_3 increases through 90°. In contrast, only one solution is found for a given θ_2 in the range $90^\circ < \theta_2 < 180^\circ$. All the solutions are also very small, of the order of a few Burgers vectors. Changing θ_2 causes $\hat{l}_2$ to change by less than one order of magnitude. Finally, the crack lengths increase with the pile-up lengths in this example, although the increase is less than one order of magnitude for the total variation of $\sim 0.15\, l_0$.

Very different crack length characteristics are predicted when the crack is on boundary three, as shown in Fig. 5. First, no solutions less than l_0 are found in the entire ranges of θ_3, l_1/l_0 and l_2/l_0 investigated. Short cracks between b and 100 b are found in the variations of θ_1 and θ_2. In at least one case, $\theta_2 = 180^\circ$, two solutions, stable and unstable, are found.

Experimental data suggest that both submicroscopic cracks (<0.05 μm) and microscopic cracks (1–50 μm) can be observed in polycrystalline metals (Regel *et al.*, 1975; Rybin and Zhukovskii, 1978). These observations are in broad agreement with the present theoretical predictions. Other mechanisms, such as that due to triple junction disclinations, however, may also be operative (Wu and Zhou, 1996b).

3.5. *Further discussion*

Future investigations would need to take into account several additional phenomena. First, frictional contact of the crack faces is likely to occur since negative mode I SIFs are predicted. Second, EGBDs can be prevented from piling up at the triple junction by trapped heterogeneities on the grain boundaries. Thus, analysis of the interactive pile-ups in the presence of these heterogeneities should also receive attention. Third, the importance of the

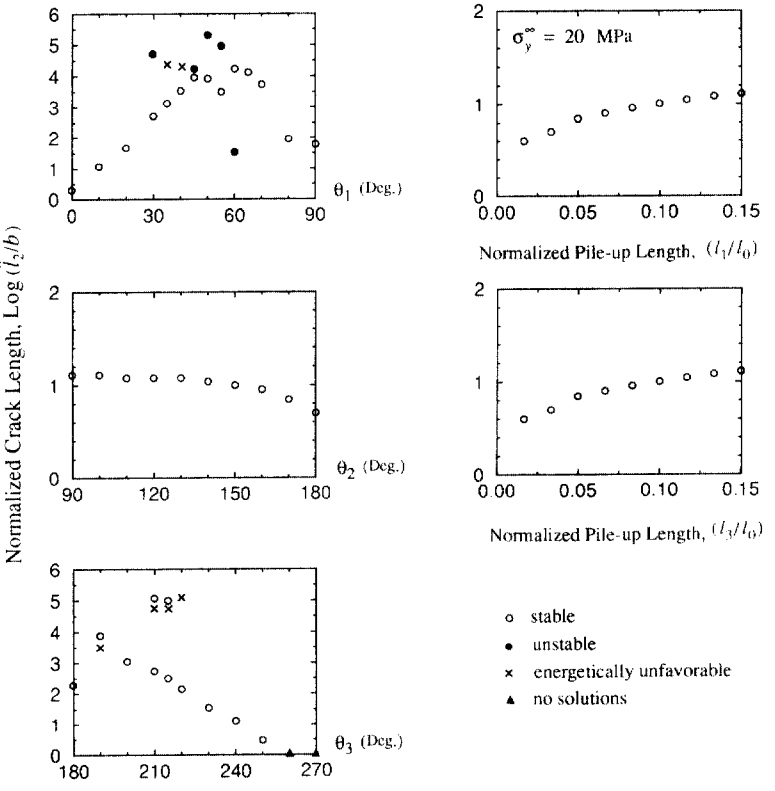

Fig. 4. Predictions of the equilibrium lengths of a crack on boundary two. The parameters investigated include the grain boundary orientations an the pile-up lengths of the dislocations. Multiple solutions corresponding to stable, unstable, and energetically unfavorable cracks are predicted for certain grain boundary orientations. No solutions can be found in some cases.

variations of the crystallographic orientations around the triple junction will need to be assessed, as already mentioned in Section 1. Fourth, whether a crack is more likely to nucleate on one or another of the three boundaries is not investigated in this paper. This can be done by comparing the values of $E_g - E_c$ in (34). Moreover, the possibility of crack branching is yet to be investigated. Finally, the present results show that the crack lengths span at least five orders of magnitude. It remains to study the statistical characteristics of the crack length distributions in a random polycrystal.

4. CONCLUSIONS

A model is developed for computing the SIFs of a triple junction crack interacting with EGBDs piling up at the head of the crack. The formulation takes into account the stress redistribution due to the crack formation as well as the rearrangement of the EGBDs. Plane strain is assumed. The EGBDs are assumed to have Burgers vectors tangential to the grain boundary planes. Furthermore, a crack nucleation model is proposed in which the energy of the crack system is used to determine whether nucleation of the crack is favorable. The stability of the predicted equilibrium crack is assessed by examining the second order derivative of the crack energy with respect to the crack length.

Numerical results show that: (i) the SIFs display extrema as well as positive, zero and negative values as the orientations are changed, suggesting the existence of favorable and unfavorable sites for crack nucleation or growth in a random polycrystal, (ii) small EGBD populations around the triple junction may also generate large SIFs, (iii) longer EGBD pile-ups do not necessarily create larger SIFs, (iv) both K_I and K_{II} generally decrease with increase in crack length but exceptions occur when the crack is sufficiently long to allow the applied tension to have a dominant effect, and (v) the dislocation populations may

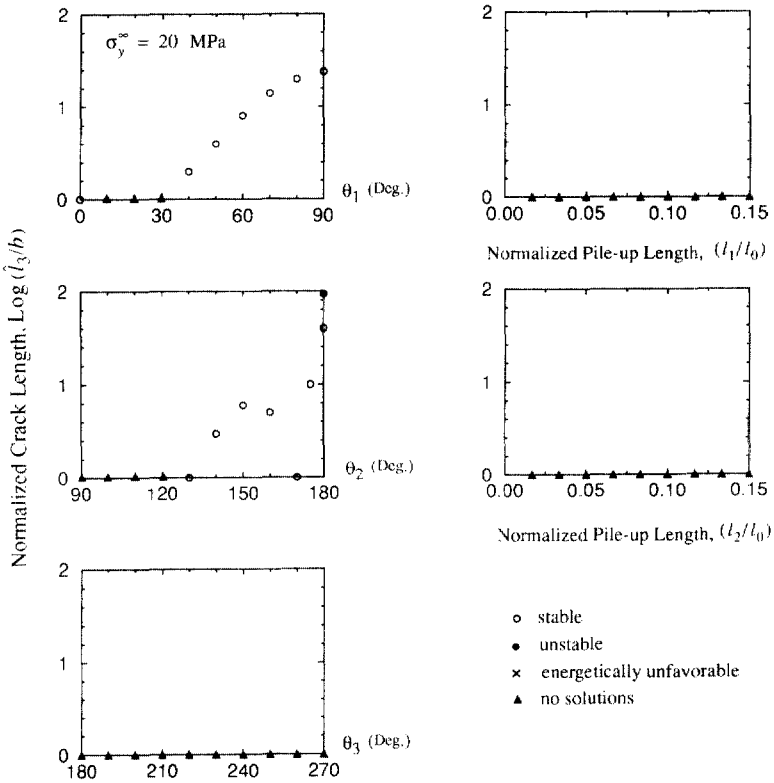

Fig. 5. Predictions of the equilibrium lengths of a crack on boundary three. The parameters investigated include the grain boundary orientations and the pile-up lengths of the dislocations. No solutions can be found for the variations of θ_3 and l_1, l_2.

decrease as the crack length increases, which can be interpreted as the admission of dislocations into and their redistribution within the crack, or the reabsorption of dislocations at the grain boundary sources.

Analysis of the equilibrium crack lengths shows that: (i) a multiplicity of crack length solutions may exist for specific combinations of the grain boundary orientations, including stable, unstable, and energetically unfavorable solutions, (ii) solutions may not be found at all, (iii) the predicted crack dimensions range from the submicroscopic to the microscopic scale, i.e., from several Burgers vectors to the order of the grain boundary length, and (iv) the stability characteristics of the cracks are highly dependent on the underlying microstructure, e.g., the boundary on which the crack is located and the grain boundary orientations.

Acknowledgements—The authors gratefully acknowledge the financial support of the National Science Foundation (Grant No. CMS-9523028), and the Center for Materials Research and Analysis, University of Nebraska-Lincoln.

REFERENCES

Gerasoulis, A. (1982) The use of piecewise quadratic polynomials for the solution of singular integral equations of Cauchy Type. *Computers and Mathematics with Applications* **8,** 15–22.

Gutkin, M. Yu and Ovid'ko, I. A. (1994) Disclinations, amorphization and microcrack generation at grain boundary junctions in polycrystalline solids. *Philosophical Magazine* **A70,** 561–575.

He, M. Y. and Hutchinson, J. W. (1989) Kinking of a crack out of an interface. *Journal of Applied Mechanics* **56,** 270.

Hirth, J. P. and Lothe, J. (1982) *Theory of Dislocations*, 857 pp. John Wiley and Sons, New York.

Lo, K. K. (1978) Analysis of branched cracks. *Journal of Applied Mechanics* **45,** 797–802.

Muskhelishvili, N. I. (1953) *Some Basic Problems of the Mathematical Theory of Elasticity*, 704 pp. Noordhoff, Groningen.

Nazarov, A. A. (1994) On the role of non-equilibrium grain-boundary structure in the yield and flow stress of polycrystals. *Philosophical Magazine* **A69,** 327–340.

Nazarov, A. A., Romanov, A. E. and Valiev, R. Z. (1993) On the structure, stress fields and energy of non-equilibrium grain boundaries. *Acta Metallurgia et Materialia* **41,** 1033–1040.

Niu, J. and Wu, M. S. (1997) Strong interactions of morphologically complex cracks. *Engineering Fracture Mechanics* **57,** 665–687.

Picu, R. C. and Gupta, V. (1995) Crack nucleation in columnar ice due to elastic anisotropy and grain boundary sliding. *Acta Metallurgia et Materialia* **43,** 3783–3789.

Regel, V. R., Leksovskii, A. M. and Sakiev, S. N. (1975) The kinetics of the thermofluctuation-induced micro- and macrocrack growth in plastic metals. *International Journal of Fracture* **11,** 841–850.

Rybin, V. V. and Zhukovskii, I. M. (1978) Disclination mechanism of microcrack formation. *Soviet Physics, Solid State* **20,** 1056–1059.

Smith, E. and Barnby, J. T. (1967) Crack nucleation in crystalline solids. *Metal Sci. J.* **1,** 56–64.

Valdimirov, V. I. and Khanhanov, Sh. Kh. (1969) Discrete-continuous examination of dislocation pile-ups. *The Physics of Metals and Metallography* **27,** 969–975.

Wu, M. S. and Niu, J. (1995) A theoretical analysis of crack nucleation due to grain boundary dislocation pile-ups in a random ice microstructure. *Philosophical Magazine* **A71,** 831–854.

Wu, M. S. and Zhou, H. (1996a) An energy analysis of triple junction crack nucleation due to the wedging action of grain boundary dislocations. *International Journal of Fracture* **78,** 165–191.

Wu, M. S. and Zhou, H. (1996b) Analysis of a crack in a disclinated cylinder. *International Journal of Fracture* **82,** 381–319.